AFRL-AFOSR-VA-TR-2018-0308

Group-IV interband and intersubband semiconductor lasers based on SiGe nanomembranes

Roberto Paiella
TRUSTEES OF BOSTON UNIVERSITY

07/19/2018
Final Report

DISTRIBUTION A: Distribution approved for public release.

Air Force Research Laboratory
AF Office Of Scientific Research (AFOSR)/ RTB1
Arlington, Virginia 22203
Air Force Materiel Command

DISTRIBUTION A: Distribution approved for public release.

REPORT DOCUMENTATION PAGE

Form Approved
OMB No. 0704-0188

The public reporting burden for this collection of information is estimated to average 1 hour per response, including the time for reviewing instructions, searching existing data sources, gathering and maintaining the data needed, and completing and reviewing the collection of information. Send comments regarding this burden estimate or any other aspect of this collection of information, including suggestions for reducing the burden, to Department of Defense, Executive Services, Directorate (0704-0188). Respondents should be aware that notwithstanding any other provision of law, no person shall be subject to any penalty for failing to comply with a collection of information if it does not display a currently valid OMB control number.
PLEASE DO NOT RETURN YOUR FORM TO THE ABOVE ORGANIZATION.

1. REPORT DATE *(DD-MM-YYYY)*
09-08-2018

2. REPORT TYPE
Final Performance

3. DATES COVERED *(From - To)*
30 Sep 2014 to 30 Apr 2018

4. TITLE AND SUBTITLE
Group-IV interband and intersubband semiconductor lasers based on SiGe nanomembranes

5a. CONTRACT NUMBER

5b. GRANT NUMBER
FA9550-14-1-0361

5c. PROGRAM ELEMENT NUMBER
61102F

6. AUTHOR(S)
Roberto Paiella, Max Lagally

5d. PROJECT NUMBER

5e. TASK NUMBER

5f. WORK UNIT NUMBER

7. PERFORMING ORGANIZATION NAME(S) AND ADDRESS(ES)
TRUSTEES OF BOSTON UNIVERSITY
1 SILBER WAY
BOSTON, MA 02215-1390 US

8. PERFORMING ORGANIZATION REPORT NUMBER

9. SPONSORING/MONITORING AGENCY NAME(S) AND ADDRESS(ES)
AF Office of Scientific Research
875 N. Randolph St. Room 3112
Arlington, VA 22203

10. SPONSOR/MONITOR'S ACRONYM(S)
AFRL/AFOSR RTB1

11. SPONSOR/MONITOR'S REPORT NUMBER(S)
AFRL-AFOSR-VA-TR-2018-0308

12. DISTRIBUTION/AVAILABILITY STATEMENT
A DISTRIBUTION UNLIMITED: PB Public Release

13. SUPPLEMENTARY NOTES

14. ABSTRACT
This project has been aimed at the development of mid- and far-infrared laser active materials based on the group-IV semiconductors Si, Ge, and SiGe (the leading materials platform of microelectronics). Because of their intrinsic CMOS compatibility, group-IV diode lasers have significant technological potential, including applications of high relevance to the DoD mission. Their implementation, however, is severely complicated by the indirect-bandgap nature of Si(Ge). Our approach to address this challenge has
been based on the use of group-IV nanomembranes (NMs) in two novel ways: (1) the formation of directbandgap Ge through the introduction of large biaxial tensile strain in mechanically stressed Ge NMs, and
(2) the development of high-quality SiGe THz quantum cascade structures consisting of strain-engineered multiple-quantum-well NMs.
Our main accomplishments in the first thrust of the project include the demonstration of strong strainenhanced photoluminescence and the formation of population inversion in (near-) direct-bandgap Ge NMs.
Furthermore, we have developed photonic-crystal cavities fully compatible with the flexibility requirements of these mechanically stressed NMs, leading to the measurement of pronounced emission resonances associated with the cavity modes. In the second thrust, we have developed a novel fabrication process for the growth of SiGe quantum wells of unprecedented crystalline quality, based on the use of strain-relaxed NM templates. With this process, we have measured THz intersubband absorption spectra with record narrow linewidths for the SiGe materials system, and we have developed SiGe quantum-well infrared photodetectors (QWIPs) providing improved responsivity compared to otherwise identical devices grown on a rigid Si substrate. Finally, we have also reported the initial observation of THz intersubband electroluminescence from simil

15. SUBJECT TERMS
nanomembranes, THz quantum cascade lasers, semiconductor lasers, SiGe

DISTRIBUTION A: Distribution approved for public release.

16. SECURITY CLASSIFICATION OF:			17. LIMITATION OF ABSTRACT	18. NUMBER OF PAGES	19a. NAME OF RESPONSIBLE PERSON
a. REPORT	b. ABSTRACT	c. THIS PAGE			POMRENKE, GERNOT
Unclassified	Unclassified	Unclassified	UU		**19b. TELEPHONE NUMBER** *(Include area code)* 703-696-8426

Standard Form 298 (Rev. 8/98)
Prescribed by ANSI Std. Z39.18

DISTRIBUTION A: Distribution approved for public release.

FINAL REPORT

Contract/Grant Title: Group-IV Interband and Intersubband Semiconductor Lasers Based on SiGe Nanomembranes

Contract/Grant #: FA9550-14-1-0361

Reporting Period: 9/30/14 to 4/1/18

Principal Investigators: Prof. Roberto Paiella (Boston University) and Prof. Max G. Lagally (University of Wisconsin – Madison)

Program Manager: Dr. Gernot Pomrenke

Technical Report:

This project has been aimed at the development of mid- and far-infrared laser active materials based on the group-IV semiconductors Si, Ge, and SiGe (the leading materials platform of microelectronics). Because of their intrinsic CMOS compatibility, group-IV diode lasers have significant technological potential, including applications of high relevance to the DoD mission. Their implementation, however, is severely complicated by the indirect-bandgap nature of Si(Ge). Our approach to address this challenge has been based on the use of group-IV nanomembranes (NMs) in two novel ways: (1) the formation of direct-bandgap Ge through the introduction of large biaxial tensile strain in mechanically stressed Ge NMs, and (2) the development of high-quality SiGe THz quantum cascade structures consisting of strain-engineered multiple-quantum-well NMs. Our accomplishments in both thrusts are summarized below.

1. Interband optical gain media based on tensilely strained nanomembranes

Several theoretical studies have long predicted that Ge can be converted into a direct-bandgap semiconductor through the introduction of biaxial tensile strain larger than about 1.9 % [1]. As a result, its interband radiative efficiency can be significantly improved, and eventually optical gain can be established under realistic pumping conditions. At the same time, in the presence of similar strain levels the Ge direct-bandgap energy is also red-shifted into the short-wave mid-infrared spectral region beyond 2 μm, where a wide range of imaging and biochemical sensing applications exists that could benefit strongly from an integrated lab-on-a-chip device platform.

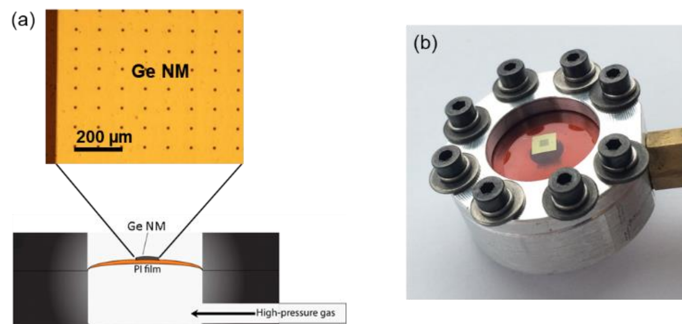

Fig. 1. Mechanically stressed Ge NMs. (a) Schematic illustration of the experimental setup used to introduce biaxial tensile strain in the NMs. A top-view optical micrograph of a NM bonded onto a PI film is also shown. The periodic black dots are etchant access holes, used to facilitate the Ge NM release from its GOI substrate. (b) Photograph of the sample mount.

DISTRIBUTION A: Distribution approved for public release.

Our prior work has shown that these relatively high strain levels can be obtained (without extended-defect formation) through the application of mechanical stress in sufficiently thin Ge NMs [2-4]. These NMs are fabricated by releasing the Ge template layer of a commercial germanium-on-insulator (GOI) substrate with a selective wet etch of the underlying oxide layer. In order to measure their strain-dependent optical properties, the NMs are then transferred onto a flexible film of polyimide (PI) and mounted in a pressure cell [Fig. 1]. With this approach, we have reported strong strain-enhanced photoluminescence (PL) and the formation of population inversion in (near-) direct-bandgap Ge [2, 3]. Furthermore, we have developed grating-coupled strained-Ge NMs producing PL emission peaked at wavelengths as long as 2.4 μm [4].

1.1 *Flexible nanomembrane photonic-crystal cavities*

Subsequent work has focused on the development of optical cavities compatible with the mechanical flexibility of these NM active materials. The key challenge in this effort has been related to the nanoscale thickness of the NMs, which is too small to provide the required in-plane waveguiding of the (predominantly TM-polarized) emitted light. As a result, additional guiding layers must be added to the NMs, without at the same time compromising their mechanical flexibility (which is essential to enable gain through straining). This challenge has been addressed with the device geometry shown schematically in Fig. 2(a), where a periodic array of dielectric columns is deposited on the NM [5]. These arrays can be made thick enough and with sufficiently large average refractive index to produce strong optical waveguiding. At the same time, if their periodicity matches the emission wavelength, they can also provide vertical outcoupling and in-plane optical feedback of the emitted light, by first and second-order diffraction, respectively. Finally, by virtue of their disconnected geometry, the same arrays do not limit the maximum strain that can be introduced in the underlying NM (at least in the regions between neighboring pillars).

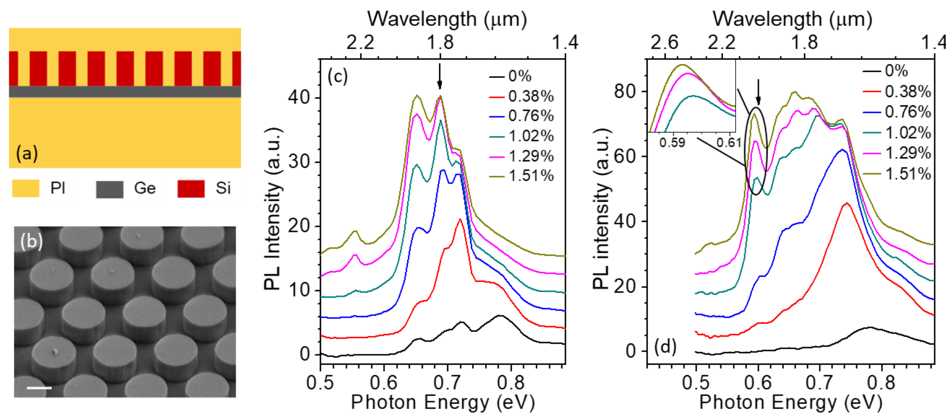

Fig. 2. Flexible photonic-crystal cavities for tensilely strained Ge NMs. (a) Schematic device cross section. (b) SEM image of a Si-pillar array before transfer onto a Ge NM on PI. The scale bar is 500 nm. (c), (d) Strain-resolved room-temperature PL spectra of two samples with different column periods *a* and diameters D: (c) *a* = 1060 nm, D = 850 nm; (d) *a* = 1340 nm, D = 950 nm. Inset of (d): zoom-in of the features within the black ellipse, showing strain tuning of the cavity modes. The arrow in each plot indicates the calculated photon energy of the main TM-polarized cavity resonance.

In the course of the project, the device geometry just described has been implemented with a novel fabrication process based on direct NM assembly [5]. In this process, an array of Si columns embedded in a flexible PI film is patterned in the template layer of a commercial Si-on-insulator (SOI) wafer, released from its native substrate with a selective wet etch, and then transferred onto a previously prepared Ge NM on PI. The resulting pillars have extremely smooth sidewalls [Fig.

DISTRIBUTION A: Distribution approved for public release.

2(b)] and therefore can be expected to provide minimal optical-scattering losses. Furthermore, because they are based on single-crystal Si, they also feature negligible absorption losses at the strained-Ge emission wavelength.

A large increase and red shift in PL emission with increasing tensile strain was once again observed with these devices, indicating a similar degree of mechanical flexibility as in the bare Ge NMs of our prior work. Representative results are shown in Figs. 2(c) and 2(d) for two 50-nm-thick Ge NMs coated with arrays of different periods. In fact, a significantly larger enhancement in PL efficiency is obtained with these devices [up to 12× in Fig. 2(d)] compared to bare NMs, due to the efficient vertical outcoupling of the TM-polarized emission produced by the column array. Furthermore, a complex pattern of relatively narrow features is observed in the PL spectra of Fig. 2, associated with different modes of the photonic-crystal cavity provided by the pillars. The spectral positions of these features are in good agreement with numerical simulations of the photonic-crystal band structures [5], and can be tuned by varying the array period and the applied strain [inset of Fig. 2(d)].

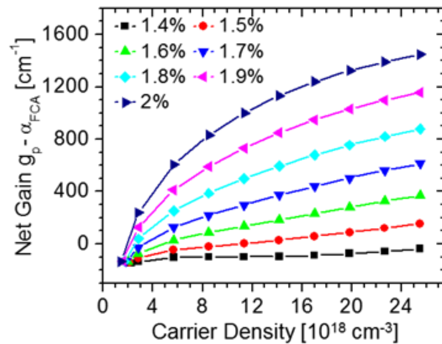

Fig. 3. Peak gain coefficient of undoped Ge (including the effect of free-carrier absorption), computed as a function of injected carrier density for different strain values [5]. For the NM cavity geometry of Fig. 2, the threshold gain required for lasing is estimated to be a few 100 cm^{-1} (if all relevant loss mechanisms are properly minimized). These simulation results therefore indicate that such threshold can be reached for strain values larger than about 1.6 % biaxial. The larger the strain, the smaller the required density of injected carriers, as expected based on the corresponding decrease in direct versus indirect bandgap energy.

These results demonstrate that ultrathin NM active layers can be effectively coupled to an optical cavity while still preserving their mechanical flexibility, which is a key requirement for the development of strain-enabled Ge NM lasers. At the same time, however, the cavity resonances of Figs. 2(c) and 2(d) are relatively broad (with quality factors of less than 100), and no evidence of spectral narrowing with increasing PL pump intensity or strain was observed in these measurements. In contrast, numerical simulations of the lasing condition for the same devices indicate that, at the highest measured strains, the NMs are already expected to be pumped near threshold [Fig. 3] [5]. We believe that the reason for this discrepancy is the presence of excess optical losses due to scattering from crystalline defects in the NM material. Such defects can be seen in microscope images and appear to originate from the GOI wafer used to fabricate the NMs. The implication is that the GOI structural quality is of critical importance to enable further progress.

1.2 *Novel substrates for Ge-nanomembrane fabrication*

Because at present GOI is not commercially available in higher-quality wafers, we have also investigated alternative approaches for the Ge NM fabrication. After exploring wafer bonding and bond-and-etch-back methods, we have concluded that the most promising approach involves growing Ge on III-V wafers. Ge is essentially lattice matched to GaAs and AlAs, and AlAs can act as a release layer because it can be etched differentially from GaAs or Ge. We have developed processing methods for the fabrication of large-area Ge NMs of various thicknesses, by careful CVD growth of Ge on AlAs/GaAs heterostructures [Fig. 4(a)] and then using a combination of known recipes for the selective etch of the AlAs release layer and transfer of the Ge NMs on a new

DISTRIBUTION A: Distribution approved for public release.

substrate [Fig. 4(b)]. A III-V MOVPE reactor has been redesigned to allow for Ge growth, and optimized growth conditions have been identified for Ge films. Structural characterization measurements show promising results regarding the materials quality of the resulting NMs [Fig. 4(c)].

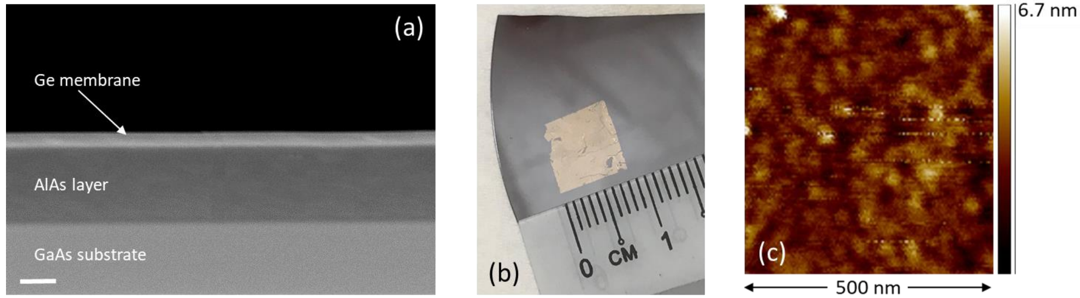

Fig. 4. Fabrication of Ge NMs from III-V substrates. (a) Cross-sectional SEM image of a 65-nm Ge film grown on an AlAs/GaAs substrate. The scale bar is 200 nm. (b) Optical image of a Ge NM released from a similar epitaxial structure. (c) AFM image showing the NM morphology after transfer onto a Si substrate. The RMS roughness is about 2 nm.

1.3 *Strain-tunable light emission from III-V nanomembranes*

As an extension of the work above, we have also investigated the use of mechanical stress in NMs to shift the emission spectrum of traditional III-V semiconductor laser media, specifically InGaAs [6]. This capability also has significant technological implications, as a means to develop dynamically tunable lasers with ultrawide tunability of their output wavelength. At present, the operation of tunable diode lasers typically relies on shifting the reflectivity spectrum of a grating mirror or external cavity. As a result, the maximum achievable tuning range is necessarily limited to a fraction of the gain bandwidth, normally on the order of a few ten nanometers for standard near-infrared devices. In contrast, the dynamic introduction of strain in NMs allows shifting the entire gain spectrum, potentially by significantly larger amounts.

The experimental samples used in this effort are based on a 100-nm-thick $In_{0.53}Ga_{0.47}As$ film lattice-matched on an $In_{0.52}Al_{0.48}As$ layer on InP (grown by MBE at Sandia National Lab). As in our prior work, the InGaAs film is released from the underlying materials with a selective wet etch to form a free-standing NM, which is then transferred and bonded onto a PI film and finally mounted in the pressure cell of Fig. 1. Figure 5(a) shows several PL spectra measured with such a NM for different values of the applied gas pressure. A large red shift in peak emission wavelength with increasing strain is observed, by more than 230 nm at the highest applied pressure of 80 psi. The corresponding biaxial tensile strain introduced in the NM reaches a maximum value of about 1% [Fig. 5(b)], as measured by X-ray diffraction (XRD). The experimental wavelengths of peak emission plotted as a function of strain are also in good agreement with the theoretical strain variations of the InGaAs band gap [Fig. 5(c)], computed by standard deformation-potential theory [7].

These results suggest a new promising application area of NM strain engineering, aimed at the development of diode lasers with record large dynamic tunability of the emission wavelength, for use in optical communications, spectroscopy and sensing, etc.. Practical device configurations may be envisioned by replacing the pressure cell with piezoelectric or MEMS actuators.

DISTRIBUTION A: Distribution approved for public release.

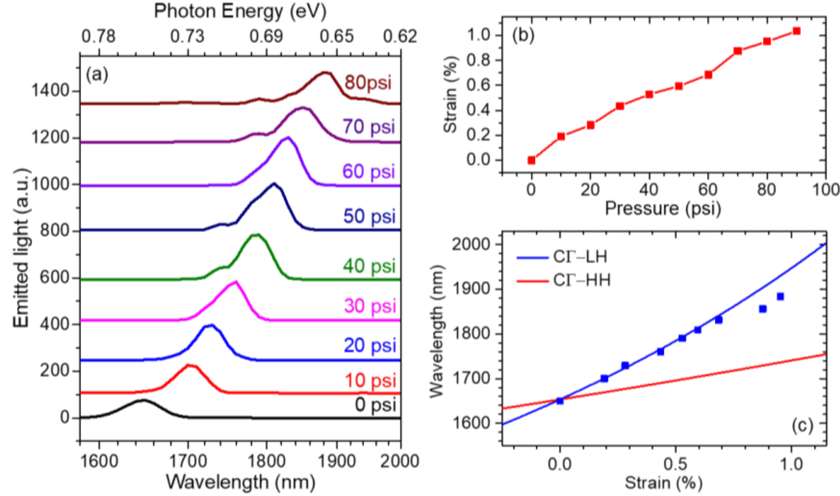

Fig. 5. Strain-tunable light emission from InGaAs NMs. (a) Room-temperature PL spectra of a 100-nm-thick $In_{0.53}Ga_{0.47}As$ NM at different pressures. (b) Biaxial tensile strain in the same NM measured as a function of pressure by XRD. (c) Solid-lines: calculated bandgap wavelengths between the conduction band and the strain-split heavy-hole (HH) and light-hole (LH) valence bands of $In_{0.53}Ga_{0.47}As$ plotted as a function of biaxial strain. Symbols: wavelengths of peak emission obtained from the PL spectra of (a).

2. Intersubband active materials based on strain-engineered SiGe quantum-well nanomembranes

Intersubband (ISB) optoelectronic devices based on SiGe quantum wells (QWs) provide a promising platform to extend the reach of silicon photonics to a wide range of imaging and sensing applications at mid- and far-infrared wavelengths. By virtue of their nonpolar nature, SiGe quantum cascade structures are also potentially capable of cryogenic-free operation across the entire THz spectrum, unlike existing GaAs THz lasers. The development of these devices, however, has so far been hindered by the large lattice mismatch between Si and Ge, which results in large densities of material defects in SiGe QWs grown on rigid epitaxial substrates [8].

To address this challenge, we have developed a novel fabrication process for the growth of high-quality SiGe QWs, based on NM strain engineering. In this process, shown schematically in Fig. 6, a few periods of the desired SiGe QW structure (with overall thickness well below the threshold for plastic deformation) are initially grown on a SOI wafer [Figs. 6(a)-(b)]. The resulting epitaxial stack is then released to form a NM by etching the underlying SiO_2 layer. In the process, the internal stress due to lattice mismatch is relaxed via elastic strain sharing among the various layers [Fig. 6(c)]. The end result is therefore a lattice-matched NM that can be used for the subsequent strain-compensated growth of an arbitrary number of QW periods without any strain accumulation. In the first samples developed with this approach, we have measured THz ISB absorption spectra with record narrow linewidths for the SiGe materials system, indicative of excellent crystalline quality [9].

2.1 *SiGe nanomembrane quantum well infrared photodetectors*

Subsequent activities have focused on the demonstration of SiGe quantum well infrared photodetectors (QWIPs) based on this novel fabrication process [10]. These samples provide a relatively simple ISB device structure to address the unique challenges related to the use of ultrathin NM active materials, such as the ability to obtain efficient current injection and extraction across the NM. To that purpose, before growth of the full multiple-QW layer, the strain-relaxed NMs are transferred onto a highly doped Si substrate, and an optimized anneal process is used to produce a tightly bonded Si-NM interface [Figs. 6(d)-(f)]. With this approach, we have developed

DISTRIBUTION A: Distribution approved for public release.

mesa-structure devices [Fig. 7(a)] with dark current-voltage characteristics fully consistent with carrier transport in multiple QWs [Fig. 7(b)]. Importantly, comparison with otherwise identical devices grown directly on the doped Si substrate [Fig. 7(c)] indicates that the bonded Si-NM interface has no significant effect on the electrical characteristics.

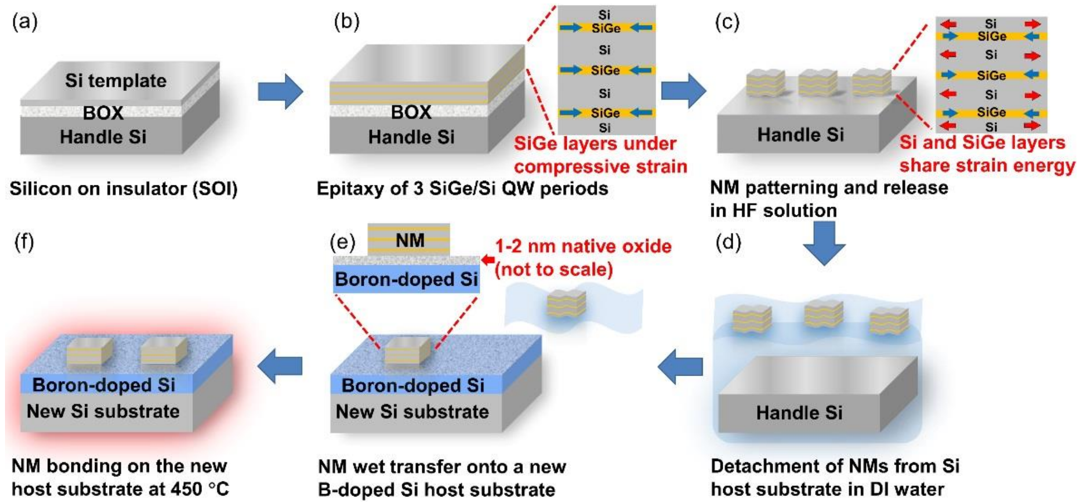

Fig. 6. Fabrication of lattice-matched SiGe/Si NM substrates. (a) SOI starting material. (b) Epitaxy of 3 SiGe/Si QW periods on SOI. The in-plane lattice of the SiGe layers is compressively strained to fit the lattice constant of the SOI Si template. (c) NM patterning by photolithography and release by etching the buried oxide layer (BOX) using HF. Upon release, all Si and SiGe layers partially relax elastically, leaving the SiGe layers less compressively strained and the Si layers slightly tensilely strained, so that the global average strain is zero. (d) Detachment of the released NMs from their host substrate upon dipping in deionized water. The NMs float to the water surface. (e) Transfer of the relaxed NM stacks to a new host, a Si substrate with a highly B-doped film and a thin native oxide layer grown via a UV ozone treatment. (f) Anneal to 450 °C to strengthen the bond between the NM and the new host substrate.

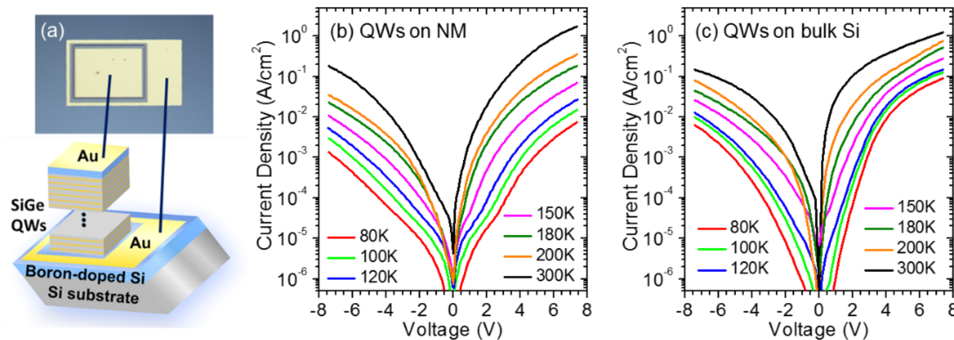

Fig. 7. Electrical properties of SiGe NM QWIPs. (a) Schematic device structure (bottom panel) and top-view optical micrograph (top panel). (b) Temperature-dependent dark electrical characteristics of a device grown on a strain-relaxed NM. (c) Temperature-dependent dark electrical characteristics of an otherwise identical device grown directly on the Si contact layer. In both plots, we observe a significant decrease in current with decreasing temperature, which indicates predominant thermal activation of the dark carrier transport through the QWs. The two devices of panels (b) and (c) also show sufficiently similar electrical characteristics that we can rule out any major detrimental effect from the bonded NM-Si interface in the former sample.

DISTRIBUTION A: Distribution approved for public release.

The optical properties of the same devices are summarized in Fig. 8. The active material of these QWIPs consists of a stack of 54 SiGe/Si QWs doped *p*-type to promote hole ISB transitions [Fig. 8(a)]. The use of *p* rather than *n*-type doping is consistent with prior work with similar structures [8], and is motivated by the exceedingly small conduction-band offsets of SiGe/Si QWs. The measured photocurrent spectra [Fig. 8(b)] show two distinct peaks, attributed to heavy-hole (HH) ISB transitions and bound-to-continuum transitions (in order of increasing photon energy). This interpretation is consistent with the calculated valence-subband structure of the active QWs [Fig. 8(a)], and is further confirmed by the polarized photocurrent spectra shown in the inset of Fig. 8(b). In particular, the long-wavelength feature is found to disappear if the input light has TE polarization (i.e., parallel to the plane of the QWs), consistent with the polarization selection rules of HH ISB transitions.

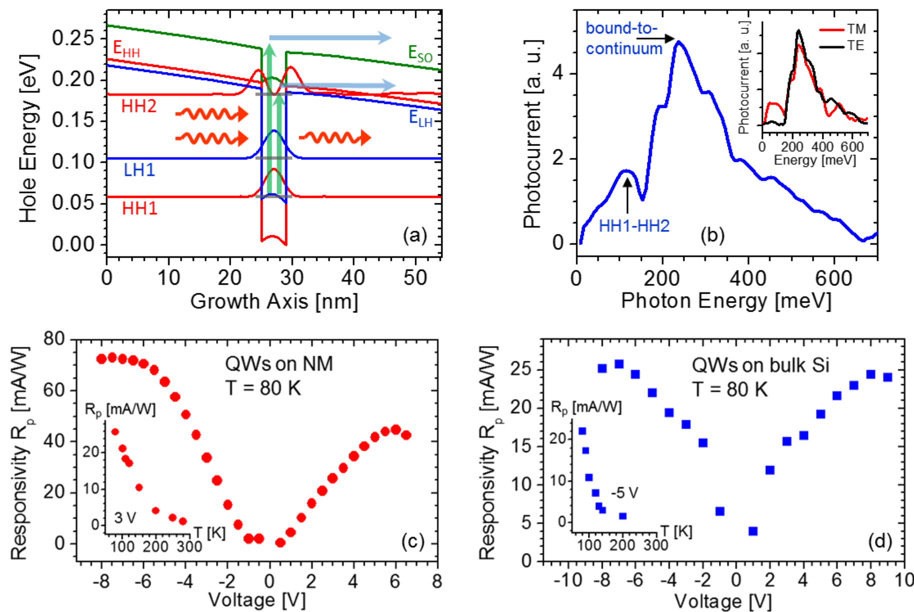

Fig. 8. Optical properties of SiGe NM QWIPs. (a) Valence-band lineup of the QWIP active material under bias, and squared envelope functions of the lowest-energy bound states. The vertical arrows indicate the main mechanisms for photocurrent generation, i.e., ISB transitions between states HH1 and HH2 (at a calculated photon energy of 122 meV) and bound-to-continuum transitions. (b) Photocurrent spectrum of a device grown on a strain-relaxed NM stack, measured with unpolarized light. The heat-sink temperature and applied voltage are 80 K and 3 V, respectively. Inset: photocurrent spectra of the same device measured with TM- and TE-polarized light. (c) and (d) Measured peak responsivity of (c) a NM QWIP and (d) a nearby device grown directly on the Si contact layer, plotted as a function of applied voltage for a heat-sink temperature of 80 K. The inset in each panel shows the peak responsivity of the corresponding device plotted as a function of temperature at fixed bias voltage.

Finally, in Fig. 8(c) we plot the peak responsivity of the same NM QWIP at 80 K as a function of bias voltage, showing a maximum value of about 73 mA/W. As shown in the inset of the same figure, the photocurrent can be resolved up to about 280 K. In Fig. 8(d) we plot the same data measured with a nearby QWIP grown directly on the Si contact layer. These plots illustrate the best performance observed with both types of devices. The bulk-grown device of Fig. 8(d) exhibits the same qualitative behavior as the NM QWIP of Fig. 8(c). Its maximum responsivity, however, is noticeably smaller, by up to a factor of over 2, consistent with the higher structural quality of

DISTRIBUTION A: Distribution approved for public release.

the strain-compensated QWs grown on the NMs. At the same time, the data of Fig. 8(c) are also comparable to or better than prior reports of SiGe QWIPs based on QWs of similar thicknesses and compositions [11-13] (albeit grown by molecular beam epitaxy, which generally provides superior control of the QW growth parameters). These results therefore fully demonstrate the feasibility and potential advantages of electrically injected ISB devices grown on strain-relaxed NM stacks.

2.2 *THz intersubband light emission from SiGe multiple-quantum-well nanomembranes*

Our most recent activities have focused on using the advances just presented to demonstrate THz ISB light emission from SiGe multiple-QW NMs. The active material developed in this work consists of a simple repetition of identical *p*-doped QWs, producing the valence-band diagram shown in Fig. 9(a). Hole transport in this structure mostly relies on tunneling from the ground-state subband (HH1) of each QW into the excited subband HH2 of the adjacent QW downstream. Intersubband light emission can then be produced through the radiative decay from this excited subband into the lower-energy states LH1 and HH1 of the same well, before the next tunneling event. While this design cannot provide population inversion, it is particularly convenient for the initial demonstration of ISB light emission because of its inherent simplicity and large tolerance to variations in layer thicknesses and compositions.

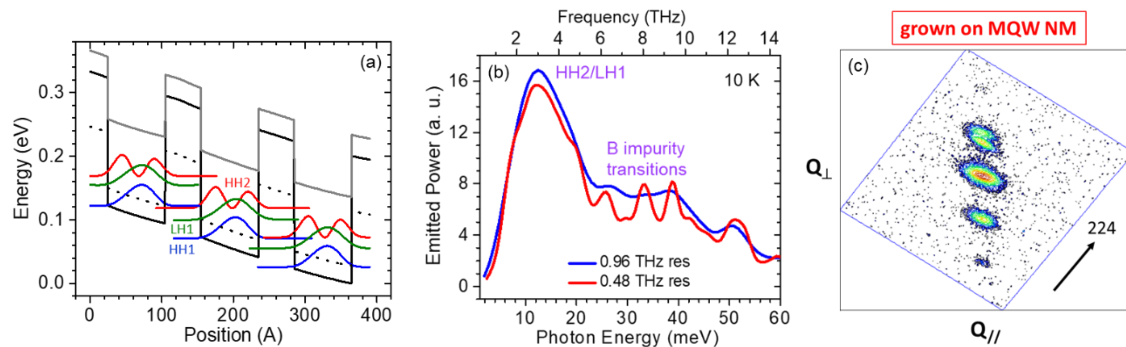

Fig. 9. THz ISB light emission from SiGe multiple-QW NMs. (a) Valence-band diagram of the QW structure used in this work, which consists of 50 repetitions of 5-nm Si barriers and 8-nm $Si_{0.72}Ge_{0.28}$ wells (nominal values). (b) Electroluminescence spectra measured with a device at a heat-sink temperature of about 10 K, for two different values of the FTIR spectrometer resolution. The emission peak near 3 THz is attributed to hole ISB transitions between the HH2 and LH1 bound states of each QW. (c) HRXRD reciprocal-space map measured along the (224) direction.

Figure 9(b) shows electroluminescence spectra measured with a mesa-structure device based on this active material, for two different values of the FTIR spectrometer resolution. For these measurements, the mesa top metal contact was patterned in the shape of a grating to promote outcoupling of the in-plane emitted QW luminescence. The device was mounted in a liquid-He continuous-flow cryostat, and THz emission was detected up to a maximum temperature of about 70 K. The main emission peak observed in these spectra is centered at a photon energy of about 12 meV (3-THz frequency), which is in reasonably good agreement with the calculated HH2-LH1 transition energy of 15 meV [Fig. 9(a)]. The narrow features in the 6-10 THz range observed in the high-resolution spectrum are instead due to impurity transitions from the B dopants, which have been reported previously in similar QWs [14].

Finally, Fig. 10 shows high-resolution X-ray diffraction (HRXRD) data measured with a subsequent sample, based on the same active-material design but grown on a further optimized

DISTRIBUTION A: Distribution approved for public release.

NM substrate [15]. Specifically, this NM consists of a Si/SiGe/Si trilayer structure again designed to produce full strain compensation in the overgrown QWs, but with significantly larger thicknesses compared to the well and barrier layers. The key advantage of this approach is that it does not require any thinning of the SOI Si template layer to match the desired barrier thickness, which is difficult to do reproducibly. As shown in Fig. 10(a), the HRXRD superlattice peaks measured with this sample (red trace) are substantially sharper than those measured with identical QWs grown on the supporting Si substrate (blue trace). The red trace is also significantly shifted toward higher values of 2theta, consistent with the elastic relaxation of the trilayer NM substrate. The superior structural quality of the QWs grown on the NM is further confirmed by comparing the reciprocal-space map of Figs. 10(b) and 10(c). Coherent growth of the QWs on the trilayer NM is inferred from Fig. 10(b), whereas Fig. 10(c) indicates substantial plastic relaxation in the QWs grown on the Si substrate. The present NM sample also compares favorably with the active material of Fig. 9 [see Fig. 9(c)], which was grown on a "standard" multiple-QW NM template.

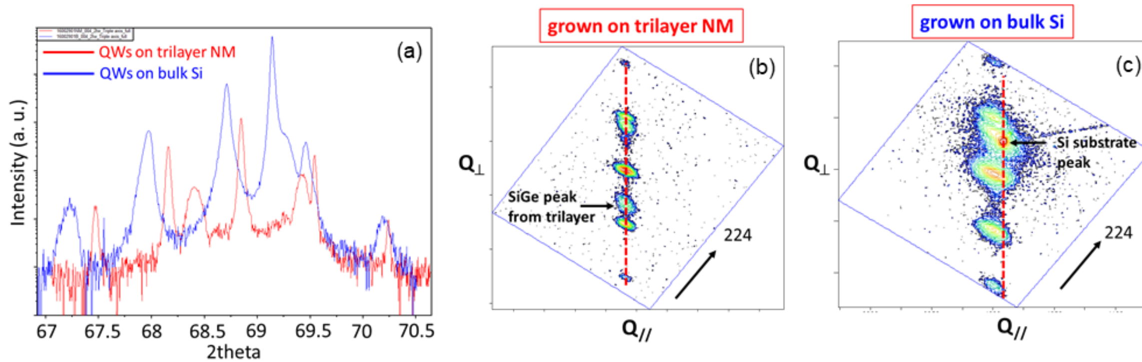

Fig. 10. HRXRD results for QWs grown on a NM trilayer substrate transferred onto a Si host wafer, and for the same active material grown simultaneously on the host wafer. The strain-relaxed NM substrate consists of a $Si/Si_{0.80}Ge_{0.20}/Si$ heterostructure with 25/80/25 nm thicknesses, giving the same average Ge composition as the overgrown QWs. (a) Omega/2theta scans along the (004) direction measured with both multiple-QW layers. (b), (c) HRXRD reciprocal-space maps measured along the (224) direction for heterostructures grown on the NM and bulk Si areas, respectively.

Unfortunately, the HRXRD data of Fig. 10 also indicate that the barrier thicknesses in this sample are significantly larger than the target value (7.1 versus 5 nm). As a result, interwell tunneling transport is severely reduced, and no evidence of ISB light emission could be observed in the electroluminescence spectra. In any case, the results shown in Fig. 10 provide the strongest evidence to date of the benefits of NM strain engineering for the growth of SiGe QW structures of unprecedented crystalline quality, and therefore are promising for the future development of advanced devices based on these materials, including THz quantum cascade lasers.

REFERENCES:

1. For a review, see: C. Boztug, J. R. Sánchez Pérez, F. Cavallo, M. G. Lagally, and R. Paiella, "Strained-germanium nanostructures for infrared photonics," ACS Nano 8, 3136–3151 (2014).
2. J. R. Sánchez Pérez, C. Boztug, F. Chen, F. F. Sudradjat, D. M. Paskiewicz, RB Jacobson, M. G. Lagally, and R. Paiella, "Direct-bandgap light-emitting germanium in tensilely strained nanomembranes," Proc. Natl. Acad. Sci. USA 108, 18893–18898 (2011).

DISTRIBUTION A: Distribution approved for public release.

3. C. Boztug, J. R. Sánchez Pérez, F. F. Sudradjat, RB Jacobson, D. M. Paskiewicz, M. G. Lagally, and R. Paiella, "Tensilely strained germanium nanomembranes as infrared optical gain media," Small 9, 622–630 (2013).
4. C. Boztug, J. R. Sánchez Pérez, J. Yin, M. G. Lagally, and R. Paiella, "Grating-coupled mid-infrared light emission from tensilely strained germanium nanomembranes," Appl. Phys. Lett. 103, 201114 (2013).
5. J. Yin, X. Cui, X. Wang, P. Sookchoo, M. G. Lagally, and R. Paiella, "Flexible nanomembrane photonic-crystal cavities for tensilely strained-germanium light emission," Appl. Phys. Lett. 108, 241107 (2016).
6. X. Wang, X. Cui, A. Bhat, J. L. Reno, M. G. Lagally, and R. Paiella, "Ultrawide strain-tunable light emission from InGaAs nanomembranes," in preparation.
7. L. A. Coldren, S. W. Corzine, and M. L. Mašanović, *Diode Lasers and Photonic Integrated Circuits* (John Wiley & Sons, 2012).
8. For a review, see: H. Sigg, "Intersubband transitions in Si/SiGe heterojunctions, quantum dots, and quantum wells," chapter 9 in R. Paiella, ed., *Intersubband Transitions in Semiconductor Quantum Structures* (Mc-Graw-Hill, 2006).
9. P. Sookchoo, F. F. Sudradjat, A. M. Kiefer, H. Durmaz, R. Paiella, and M. G. Lagally, "Strain-engineered SiGe multiple-quantum-well nanomembranes for far-infrared intersubband device applications," ACS Nano 7, 2326-2334 (2013).
10. H. Durmaz, P. Sookchoo, X. Cui, RB Jacobson, D. E. Savage, M. G. Lagally, and R. Paiella, "SiGe nanomembrane quantum well infrared photodetectors," ACS Photon. 3, 1978-1985 (2016).
11. R. People, J. C. Bean, C. G. Bethea, S. K. Sputz, and L. J. Peticolas, "Broadband (8–14 μm), normal incidence, pseudomorphic Ge_xSi_{1-x}/Si strained-layer infrared photodetector operating between 20 and 77 K," Appl. Phys. Lett. 61, 1122-1124 (1992).
12. P. Kruck, M. Helm, T. Fromherz, G. Bauer, J. F. Nützel, and G. Abstreiter, "Medium-wavelength, normal-incidence, p-type Si/SiGe quantum well infrared photodetector with background limited performance up to 85 K," Appl. Phys. Lett. 69, 3372-3374 (1996).
13. D. Krapf, B. Adoram, J. Shappir, A. Sa'ar, S. G. Thomas, J. L. Liu, and K. L. Wang, "Infrared multispectral detection using Si/Si_xGe_{1-x} quantum well infrared photodetectors," Appl. Phys. Lett. 78, 495-497 (2001).
14. R. Bates, S. A. Lynch, D. J. Paul, Z. Ikonić, R. W. Kelsall, P. Harrison, S. L. Liew, D. J. Norris, A. G. Cullis, W. R. Tribe, and D. D. Arnone, "Interwell intersubband electroluminescence from Si/SiGe quantum cascade emitters," Appl. Phys. Lett. 83, 4092 (2003).
15. P. Sookchoo, M. Zamiri, H. Durmaz, F. F. Sudradjat, D. E. Savage, R. Paiella, and M. G. Lagally, "Strain-engineered nanomembrane substrates for Si/SiGe heterostructures," (review) in preparation.

DISTRIBUTION A: Distribution approved for public release.

AFOSR Deliverables Submission Survey

Response ID:10091 Data

1.

Report Type

Final Report

Primary Contact Email
Contact email if there is a problem with the report.

rpaiella@bu.edu

Primary Contact Phone Number
Contact phone number if there is a problem with the report

617-353-8883

Organization / Institution name

Boston University

Grant/Contract Title
The full title of the funded effort.

Group-IV Interband and Intersubband Semiconductor Lasers Based on SiGe Nanomembranes

Grant/Contract Number
AFOSR assigned control number. It must begin with "FA9550" or "F49620" or "FA2386".

FA9550-14-1-0361

Principal Investigator Name
The full name of the principal investigator on the grant or contract.

Roberto Paiella

Program Officer
The AFOSR Program Officer currently assigned to the award

Gernot Pomrenke

Reporting Period Start Date

09/30/2014

Reporting Period End Date

04/01/2018

Abstract

This project has been aimed at the development of mid- and far-infrared laser active materials based on the group-IV semiconductors Si, Ge, and SiGe (the leading materials platform of microelectronics). Because of their intrinsic CMOS compatibility, group-IV diode lasers have significant technological potential, including applications of high relevance to the DoD mission. Their implementation, however, is severely complicated by the indirect-bandgap nature of Si(Ge). Our approach to address this challenge has been based on the use of group-IV nanomembranes (NMs) in two novel ways: (1) the formation of direct-bandgap Ge through the introduction of large biaxial tensile strain in mechanically stressed Ge NMs, and (2) the development of high-quality SiGe THz quantum cascade structures consisting of strain-engineered multiple-quantum-well NMs.

Our main accomplishments in the first thrust of the project include the demonstration of strong strain-enhanced photoluminescence and the formation of population inversion in (near-) direct-bandgap Ge NMs. Furthermore, we have developed photonic-crystal cavities fully compatible with the flexibility requirements of these mechanically stressed NMs, leading to the measurement of pronounced emission resonances associated with the cavity modes. In the second thrust, we have developed a novel fabrication process for

DISTRIBUTION A: Distribution approved for public release.

the growth of SiGe quantum wells of unprecedented crystalline quality, based on the use of strain-relaxed NM templates. With this process, we have measured THz intersubband absorption spectra with record narrow linewidths for the SiGe materials system, and we have developed SiGe quantum-well infrared photodetectors (QWIPs) providing improved responsivity compared to otherwise identical devices grown on a rigid Si substrate. Finally, we have also reported the initial observation of THz intersubband electroluminescence from similar samples.

Distribution Statement

This is block 12 on the SF298 form.

Distribution A - Approved for Public Release

Explanation for Distribution Statement

If this is not approved for public release, please provide a short explanation. E.g., contains proprietary information.

SF298 Form

Please attach your SF298 form. A blank SF298 can be found here. Please do not password protect or secure the PDF The maximum file size for an SF298 is 50MB.

SF_298.pdf

Upload the Report Document. File must be a PDF. Please do not password protect or secure the PDF . The maximum file size for the Report Document is 50MB.

Paiella_Lagally_Final_Report.pdf

Upload a Report Document, if any. The maximum file size for the Report Document is 50MB.

Archival Publications (published) during reporting period:

1. P. Sookchoo, M. Zamiri, H. Durmaz, F. F. Sudradjat, D. E. Savage, R. Paiella, and M. G. Lagally, "Strain-Engineered Nanomembrane Substrates for Si/SiGe Heterostructures," (review) in preparation.

2. X. Wang, X. Cui, A. Bhat, J. L. Reno, M. G. Lagally, and R. Paiella, "Ultrawide Strain-Tunable Light Emission from InGaAs Nanomembranes," in preparation.

3. R. Paiella and M. G. Lagally, "Optical Properties of Tensilely Strained Ge Nanomembranes," Nanomaterials, vol. 8, pp. 407–416, 2018 (INVITED REVIEW ARTICLE).

4. H. Durmaz, P. Sookchoo, X. Cui, RB Jacobson, D. E. Savage, M. G. Lagally, and R. Paiella, "SiGe Nanomembrane Quantum Well Infrared Photodetectors," ACS Photon., vol. 3, pp. 1978-1985, 2016.

5. J. Yin, X. Cui, X. Wang, P. Sookchoo, M. G. Lagally, and R. Paiella, "Flexible Nanomembrane Photonic-Crystal Cavities for Tensilely Strained-Germanium Light Emission," Appl. Phys. Lett. vol. 108, art. no. 241107, 2016.

6. X. Wang, X. Cui, J. Reno, M. Lagally, and R. Paiella, "Ultrawide Strain-Tunable Light Emission from InGaAs Nanomembranes," Compound Semiconductor Week, paper Th2A6.6, Boston (MA), May 2018.

7. H. Durmaz, P. Sookchoo, X. Cui, RB Jacobson, D. E. Savage, M. G. Lagally, and R. Paiella, "Strain-Engineered SiGe Nanomembrane Quantum-Well Infrared Photodetectors," IEEE Conference on Lasers and Electro-Optics, paper STh3I.2, San Jose (CA), May 2017.

8. X. Cui, X. Wang, A. Bhat, J. Yin, S. Y. Khor, J. Sánchez-Pérez, R. Paiella, and M. G. Lagally, "Enhancement of Luminescence from Strained-Ge Nanomembranes," MRS Fall Meeting, paper NM5.2.04, Boston (MA), Nov 2016.

9. J. Yin, X. Cui, X. Wang, M. Lagally, and R. Paiella, "Mechanically Flexible Photonic-Crystal Cavities on Strained Germanium Fabricated by Nanomembrane Assembly," IEEE Conference on Lasers and Electro-Optics, paper SM3R.1, San Jose (CA), June 2016.

10. H. Durmaz, P. Sookchoo, F. F. Sudradjat, A. M. Kiefer, M. G. Lagally, and R. Paiella, "SiGe Nanomembrane Active Materials for Far-Infrared Intersubband Devices," OSA Topical Meeting on Integrated Photonics Research (IPR), paper IT3A.5, Boston (MA), June 2015.

11. J. Yin, J. R. Sánchez-Pérez, C. Boztug, M. G. Lagally, and R. Paiella, "Infrared Light Emission from Germanium Nanomembranes with Mechanically Flexible Photonic-Crystal Cavities," OSA Topical Meeting on Integrated Photonics Research (IPR), paper IT3A.4, Boston (MA), June 2015.

12. P. Sookchoo, H. Durmaz, RB Jacobson, Y. Li, X. Cui, R. Paiella, and M. G. Lagally, "Strain Engineered Defect-Free SiGe Nanomembranes: Substrates for Epitaxial Growth of SiGe Multiple Quantum Wells," 9th International Conference on Silicon Epitaxy and Heterostructures (ICSI 9), Montreal (Canada), May 2015.

13. M. G. Lagally "Group-IV Sheet Science and Technology: Growth, Transfer, and Function," 9th International Conference on Silicon Epitaxy and Heterostructures (ICSI 9), Montreal (Canada), May 2015 (INVITED).

14. R. Paiella, "III-Nitride and Silicon-Based Materials for THz Quantum Cascade Lasers," European Microwave Conference, Workshop: "Terahertz Technologies - From Materials to Devices and Their Applications", paper WS1.06, Rome (Italy), Oct 2014 (INVITED).

New discoveries, inventions, or patent disclosures:

Do you have any discoveries, inventions, or patent disclosures to report for this period?

No

Please describe and include any notable dates

Do you plan to pursue a claim for personal or organizational intellectual property?

Changes in research objectives (if any):

None

Change in AFOSR Program Officer, if any:

None

Extensions granted or milestones slipped, if any:

A 7-month no-cost extension was granted, extending the end date of the award from 9/29/17 to 4/30/18.

AFOSR LRIR Number

LRIR Title

Reporting Period

Laboratory Task Manager

Program Officer

Research Objectives

Technical Summary

Funding Summary by Cost Category (by FY, $K)

	Starting FY	FY+1	FY+2
Salary			
Equipment/Facilities			
Supplies			
Total			

Report Document

DISTRIBUTION A: Distribution approved for public release.

Report Document - Text Analysis

Report Document - Text Analysis

Appendix Documents

2. Thank You

E-mail user

Jul 19, 2018 12:29:52 Success: Email Sent to: rpaiella@bu.edu

DISTRIBUTION A: Distribution approved for public release.